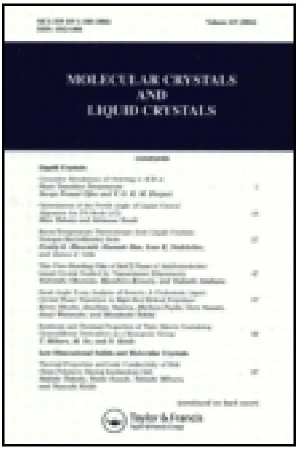

Molecular Crystals and Liquid Crystals Science and Technology. Section A. Molecular Crystals and Liquid Crystals

Publication details, including instructions for authors and subscription information:
http://www.tandfonline.com/loi/gmcl19

Image Mode Laser Projection Utilizing Twisted Nematic Liquid Crystal Technology: Model and Experiment of Amplified Spontaneous Emission

Gregory P. Crawford [a], Joel A. Firehammer [a] & Nabil M. Lawandy [b]

[a] Division of Engineering, Brown University, Providence, Rhode, Island, 02912

[b] Spectra Science Corporation, Providence, Rhode, Island

Version of record first published: 24 Sep 2006

Mol. Cryst. and Liq. Cryst., 2001, Vol. 359, pp. 341-349
Reprints available directly from the publisher
Photocopying permitted by license only

Image Mode Laser Projection Utilizing Twisted Nematic Liquid Crystal Technology: Model and Experiment of Amplified Spontaneous Emission

GREGORY P. CRAWFORD[a], JOEL A. FIREHAMMER[a] and NABIL M. LAWANDY[b]

[a]*Division of Engineering, Brown University, Providence, Rhode Island 02912 and* [b]*Spectra Science Corporation, Providence, Rhode Island*

Details of an image mode projection display are presented that utilize a twisted nematic display within the cavity of a laser. The reduction in the output efficiency of an image mode laser configuration due to amplified spontaneous emission is studied both theoretically and experimentally. It was found that in order to maximize efficiency, cavity loss should be minimized while maximizing the aspect ratio of the gain region and the optical pump rate.

Keywords: twisted nematic; lasing; amplified spontaneous emission

INTRODUCTION

The replacement of incoherent illumination sources with lasers in video projection technology has received a considerable amount of recent interest, due to the intense saturation available for all three primary colors, which results from the inherent spectral purity of lasers.[1] This unique expanded color gamut, in addition to providing colors not available to standard video projection systems, also results in perceived brightness exceeding that of a such systems with an equivalent power output.[2] We have developed a laser video projection method that is based on the image mode laser,[2] shown in Figure 1, that utilizes a twisted nematic liquid crystal display within an optical pumped laser cavity. The transverse mode of this laser creates a desired image that can be projected onto a viewing screen. This method of creating a lasing projected image has the potential advantages of higher contrast and brightness at the faceplate over the traditional method of spatial light modulation of a uniform optical source. The elimination of scanning systems results in a simpler design without mechanical parts; also, this system can potentially be adapted to full color with a single laser providing optical pumping for image mode lasers of all three primary colors.[3]

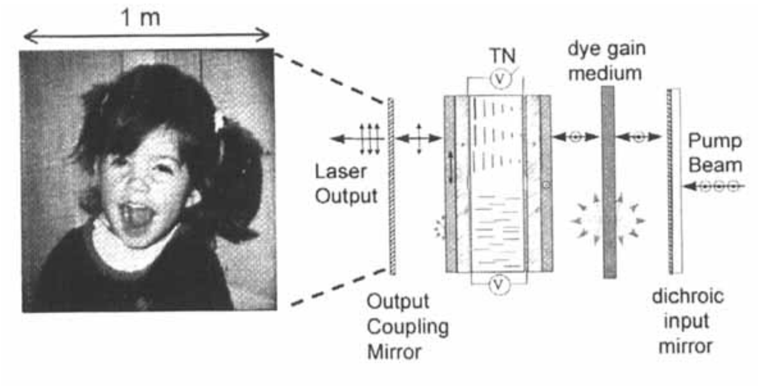

FIGURE 1: Operating principle of image mode lasers, which employs a twisted nematic (TN) spatial light modulator. The pump beam excites the entire gain medium through a dichroic mirror, which is reflective to the lasing wavelength. A quarter VGA output, monochromatic image is shown that was projected on-screen and is approximately one-meter in size.

The biggest advantage of laser based displays are of course their high degree of spectral purity, large color gamuts, and potentially bright images. The large color palette greatly expands the information bandwidth available to the human observer, thereby significantly increasing visual comprehension. Figure 2 shows a rough simulation of a full-color display using three relatively narrow laser emission lines, and from the CIE diagram, one can see that the color performance of the laser is far superior to a standard cathode-ray-tube. Miniature laser displays arguably constitute a core enabling technology for the future of head mounted display applications and immersive virtual reality, along with many compelling applications in the medical and military sector.

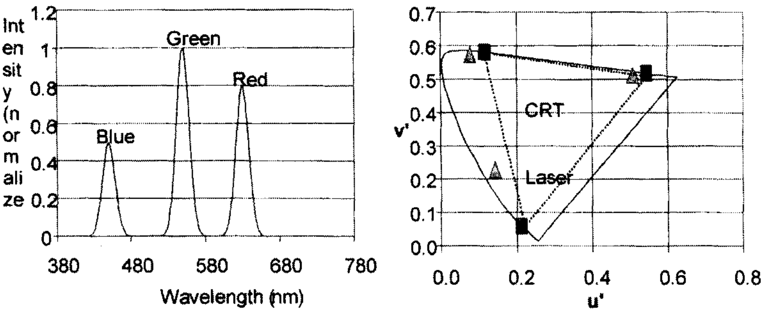

FIGURE 2: Example calculation of a full-color laser display. The spectral output functions for blue, green, and red are shown on the left and the corresponding chromaticity coordinates are shown on the right.

In this contribution we analyze how amplified spontaneous emission (ASE) can decrease output efficiency of our image mode concept shown in Figure 1, limiting the maximum useful pixelated area that can be optically excited, and how these effects can be minimized. The effects of ASE on dye laser and amplifier system have been studied in a number of papers.[3] While numerical approaches exist for general calculation of ASE in such systems, here we propose a simple analytic model for calculating ASE in the transverse direction in the low aspect ratio cavities necessary for a lasing pixel system.[3]

MODEL

A disk-shaped organic dye gain region in a laser cavity of radius R and thickness T is optically pumped with uniform intensity. The gain medium is dominated by homogeneous line broadening, and can be modeled as a two-level system. We will assume that the lasing and ASE line centers will occupy a similar frequency space, so that we may ignore any spectral overlap dependencies in the model. The intensity due to ASE at any point $\mathbf{r}_1$ in the gain medium, normalized to its saturation intensity, is given by:

$$I_{ASE}(\mathbf{r}_1) = \frac{\eta_f}{4\pi} \iiint_{\mathbf{r}_2} \frac{g(\mathbf{r}_2)}{|\mathbf{r}_2 - \mathbf{r}_1|} e^{\left[\int_{r_1}^{r_2} g(r)dr\right]} dV \qquad (1)$$

where η_f is the fluorescent quantum efficiency and $g(r)$ is the gain.

To determine how ASE influences the efficiency of a lasing pixel system, two cases will be considered: the case of all pixels in the on state, and a single pixel in the on-state at the center of an array. In this large area multi-mode cavity, the output intensity assumes a uniform profile when all pixels are turned on. So in this case the gain everywhere is constant, clamped to the round-trip losses:

$$g = \frac{\delta_c}{2 \cdot T}, \tag{2}$$

where δ_c is the total round-trip cavity loss. The gain region of interest is a small aspect ratio q disk, where $q=T/R<1$. Invoking the small angle approximation and evaluating at the center of the disk:

$$I_{ASE}(0) = \frac{\eta_f \delta_c}{4} \int_{q}^{q_0} \frac{e^{\frac{\delta_c}{2q'}}}{q'} dq', \tag{3}$$

The value q_0 is an upper bound on the integral required to account for violation of the small angle approximation at a small distance from the point. If the argument of the exponent in the integral is much greater than unity, which is true in most cases in which ASE is significant, the integral can be approximated to the first order:

$$I_{ASE}(0) = \frac{\eta_f q}{2} e^{\frac{\delta_c}{2q}}. \tag{4}$$

The efficiency at any point in the cavity can then be found by employing Rigrod's large output coupling analysis,[1] incorporated the ASE intensity into the equation for gain saturation, i.e.:

$$g = \frac{g_0}{1 + I_f + I_r + I_{ASE}}, \tag{5}$$

where I_f and I_r are the forward and reverse travelling waves normalized to I_{sat}, and g_0 is the unsaturated (small-signal) gain coefficient. Using this approach, the power extraction efficiency is given by

$$\eta_{ASE} = \frac{(1-r_o^2)}{(1+\frac{r_o}{r_i})(1-r_i r_o)}\left[1-\frac{1+\frac{\eta_f q}{2}e^{\frac{\delta_c}{2q}}}{2Tg_0/\delta_c}\right] \tag{6}$$

Equation (6) indicates that the dominant factors are cavity loss (cavity Q) and aspect ratio. A larger cavity loss (or lower Q) increases ASE because the cavity gain is clamped to a higher value, resulting in greater amplification. A smaller aspect ratio also increases ASE because an increase in radius leads to a greater path length for transverse amplification, while a decrease in thickness requires a gain increase for an equivalent gain-length product. Efficiency also increases with pump intensity because the cavity intensity scales linearly with it while ASE remains constant. These results are in agreement with the results of Haag *et. al.*[5] for calculations of ASE in a pencil-like geometry. In Figure 3 these results are plotted to demonstrate the effects of cavity Q and aspect ratio on lasing efficiency.

The second case considered is that of a single pixel is turned on at the center of the array. In this case, gain is saturated entirely by ASE since there is no laser action except at the on-state pixel. Again assuming a small aspect ratio disk, the ASE intensity can then be expressed as a function of the saturated gain value:

$$I_{ASE}(\mathbf{r}) = \frac{g_0}{g_{off}(\mathbf{r})} - 1, \tag{7}$$

where $g_{off}(\mathbf{r})$ is the gain anywhere except at the pixel. Setting the right-hand side of (1) equal to (7), the gain and ASE intensity can be found numerically. This equation was solved over a large range of conditions and was found to result in a nearly uniform gain profile; the gain value at the center of the disk when allowing for a variable gain profile differed less than 3% from the value when assuming uniform gain. This allows uniform gain to be considered an good approximate solution when solving for the gain at the pixel at the center of the disk, i.e.,

$$\frac{\eta_f q}{2}e^{\frac{g_{off}T}{q}} = \frac{g_0}{g_{off}} - 1, \tag{8}$$

which must be solved numerically for g_{off}. This value of g_{off} can then be used to solve for the efficiency of the pixel:

$$\eta_{ASE} = \frac{(1-r_o^2)}{(1+\frac{r_o}{r_i})(1-r_i r_o)}\left[1-\frac{1+\frac{\eta_f q}{2}e^{\frac{g_{off}T}{q}}}{2Tg_0/\delta_c}\right] \tag{9}$$

Note that decreasing loss leads to an increase in efficiency for an equivalent pump power and thus a linear decrease in ASE, but does not lead to the exponential decrease as in the prior case. Also, in any cavity that supports lasing, I_{ASE} must be less than the cavity intensity, so $g_{off} > g_{lase}$. This case then gives less efficiency because the exponential term is larger, so it is the limiting case for proper cavity design. These results are also shown in Figure 3.

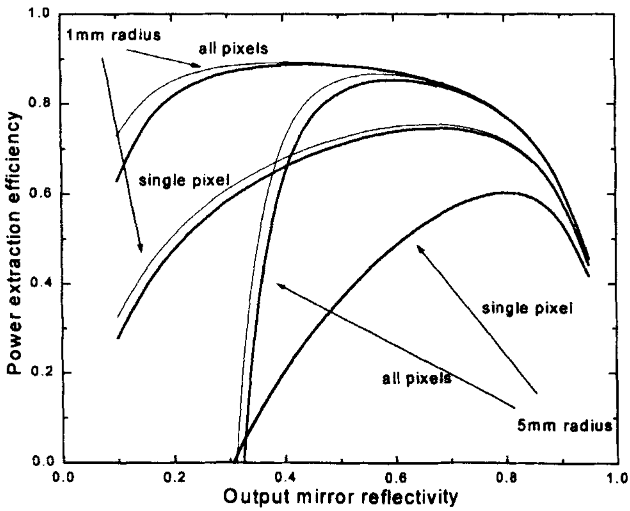

FIGURE 3: Power extraction efficiency vs. output mirror reflectivity for a 1mm and 5mm radius gain region, for all pixels on and one pixel on. The heavier lines represent the exact 3D solutions, while the lighter lines include the small angle and first-order approximations.

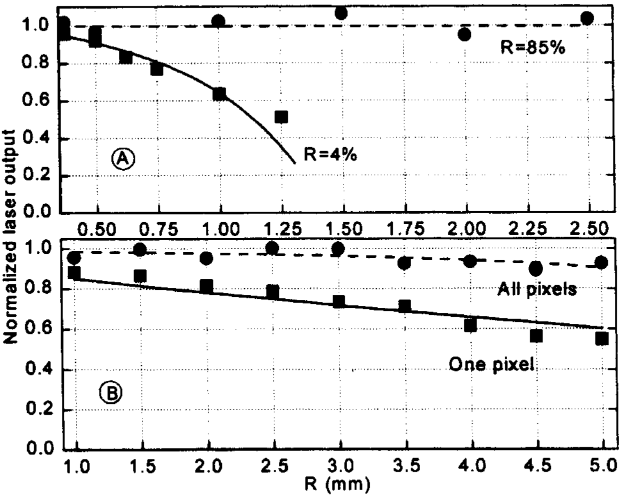

FIGURE 4: A) Measurements of the output of a non-pixelated device while varying the pump beam radius, for output coupling mirror reflectivity values of 0.04 and 0.85, with respective theoretical efficiencies. B) Measurements of the output of a single 1-mm diameter pixel turned on at the center of the pumped area while varying the pump radius. Also shown is the output of the same cavity with all pixels on, with theory.

EXPERIMENTAL RESULTS

To test the model, an experimental device was constructed using the laser dye rhodamine 6G in ethylene glycol (2.5×10^{-4} molar concentration) as a laser gain medium, circulating through a 500-micron thick dye flow cell. The dye was excited by 532-nm 7-ns pulses at 10-Hz from a frequency doubled Q-switched Nd:YAG laser through a dichroic back mirror. The PDLC used in the pixel was made from a mixture of liquid crystal TL205 and polymer PN393 (E. Merck) in ratio of 4:1 by weight, cured via ultraviolet exposure into a 10-micron thick film between two transparent conducting indium-tinoxide coated glass plates. An optical multichannel analyser was used to measure the spectra of the ASE and lasing output of the device, and confirmed that the peak of the output occurred at ~565 nm in both cases.

To test the case of all pixels turned on, the output at the center of a non-pixelated device was measured while adjusting the diameter of the pumped region. The pump power was maintained at a constant fluence of 120-mJ/cm^2, while the output energy was measured using a photodiode. Both a low and a high output-coupling mirror were used to test the effect of cavity Q on output. For the single pixel case, the output of a 1mm diameter pixel was measured while varying the pumped area diameter. A 65% reflective output mirror was device was also measured as a comparison. The results of both measurements, which show good agreement with theory, are shown in Figure 4.

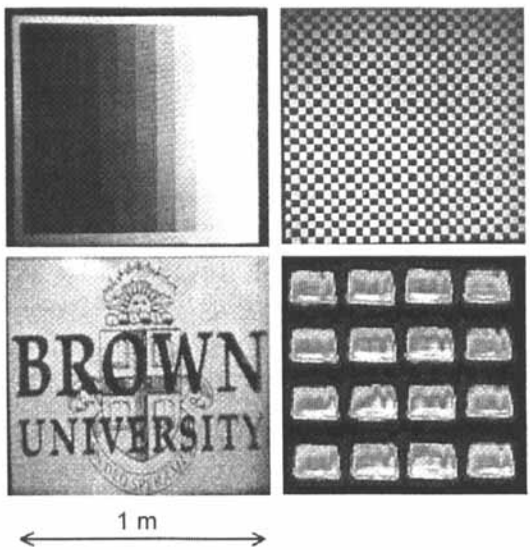

FIGURE 5: Photographs of image mode laser pictures projected onto a 1 meter diagonal screen, along with a close up of a 4×4 array imaged onto a laser beam analyzer (bottom right).

Using these results, a 300x300 resolution image mode laser was built, using Rhodamine B in a solid polymer host, and a commercial TN active matrix display as the intracavity spatial light modulator. The thickness of the gain medium was 6 mm, and the width was 9.6 mm, giving an aspect ratio of 0.625. Standard monochrome evaluation images are presented in Figure 5. Both checkerboard and total contrast evaluations were performed. The results are presented in Table 1, and are compared with both a full-color LCD projector and projection of laser radiation directly through the light valve, to determine if an image-mode laser can provide better contrast than such systems. The table indicates that a monochromatic image mode laser can provide far better contrast than a monochromatic element in the commercial LCD display system, and also provides better contrast than using a laser as a drop-in replacement for an illumination source.

Device	Total [CB]	Lm(Cd/m^2)
Image Mode	>500:1 [300:1]	32
Direct Laser	180:1 [80:1]	49
Comm. (white)	240:1 [140:1]	177
Comm. (R)	50:1 [35:1]	33
Comm. (G)	75:1 [40:1]	52
Comm. (B)	18:1 [12:1]	13

Table 1: Comparison of contrast and luminance.

Acknowledgements
This work is supported by Spectra Science Corporation, a State of Rhode Island Samuel Slater Grant, a phase II SBIR grant from the Ballistic Missile Organization, and the Air Force Office of Scientific Research.

References

[1] E.C. Haseltine, D. Ansley, 1996 *OSA Technical Digest Series, Conferences on Lasers and Electro-Optics,* **9** 69 (1996).
[2] W.K. Bohannon, *Information Display,* **8**/97 32 (1997).
[3] J.A. Firehammer, G.P. Crawford, N.M. Lawandy, *Applied Physics Letters,* **73** 590 (1998).
[4] N.M. Lawandy, J.A. Firehammer, S.D. Vartak, *Laser Focus World,* **33**/5 137 (1997).
[5] G. Haag, M. Munz, and G. Marowsky *IEEE J. Quantum Electron* **QE-19,** 1149 (1983).
[6] N.M. Lawandy, J.A. Firehammer, S.D. Vartak, G.P. Crawford, *Journal of the Society for Information Display* **5**/4 383 (1997).
[7] W.W. Rigrod, *J. Appl. Phys.* **36,** 2487 (1965).